Computers and Mathematics with Applications 61 (2011) 3711–3721

Contents lists available at ScienceDirect

Computers and Mathematics with Applications

journal homepage: www.elsevier.com/locate/camwa

Multiplicity of steady solutions in two-dimensional lid-driven cavity flows by Lattice Boltzmann Method

D. Arumuga Perumal, Anoop K. Dass *

Department of Mechanical Engineering, Indian Institute of Technology Guwahati, Guwahati-781039, India

ARTICLE INFO

Keywords:
Lattice Boltzmann Method
D2Q9 model
Two-sided square cavity
Four-sided square cavity
Bounce-back boundary condition

ABSTRACT

This work is concerned with the computation of two- and four-sided lid-driven square cavity flows and also two-sided rectangular cavity flows with parallel wall motion by the Lattice Boltzmann Method (LBM) to obtain multiple stable solutions. In the two-sided square cavity two of the adjacent walls move with equal velocity and in the four-sided square cavity all the four walls move in such a way that parallel walls move in opposite directions with the same velocity; in the two-sided rectangular lid-driven cavity flow the longer facing walls move in the same direction with equal velocity. Conventional numerical solutions show that the symmetric solutions exist for all Reynolds numbers for all the geometries, whereas multiplicity of stable states exist only above certain critical Reynolds numbers. Here we demonstrate that Lattice Boltzmann method can be effectively used to capture multiple steady solutions for all the aforesaid geometries. The strategy employed to obtain these solutions is also described.

1. Introduction

The lid-driven cavity flow is not only technically important but also of great scientific interest because it displays almost all fluid mechanical phenomena in the simplest of geometrical settings. The classical cavity problem has attracted considerable attention because its flow configuration is relevant to many industrial applications and academic research [1–3]. It is known that cavity flows arise in applications such as short-dwell coating, drug-reducing riblets in aerodynamics, removal of species from structured surfaces, mixing and flow in drying devices. A number of experimental and numerical studies have been conducted to investigate the flow field of a single-sided lid-driven cavity flow in the last several decades. The features of the single-sided lid-driven cavity flow consist of a large primary eddy and secondary corner eddies. Several flow characteristics like flow instability, corner eddies and transition to turbulence can be observed in this system. Conventional numerical solutions reveal that in a single-sided cavity flow beyond the critical Reynolds number, Hopf bifurcation takes place with the steady-flow solution becoming unstable. The single-sided lid-driven cavity flow problem was extended to two-sided lid-driven cavity by Kuhlmann and other investigators [4–9] and they have done several experiments on the two-sided lid-driven cavity with various spanwise aspect ratios. They numerically simulated the rectangular cavity flow for parallel and antiparallel motion of two of the walls and showed that a plethora of vortex patterns can be generated with different aspect ratios and directions of motion of the walls.

Many nonlinear systems give multiple steady solutions even though governing equations and boundary conditions are the same. The concept of uniqueness of numerical solution associated with the so-called well-posed nature of the problem is not applicable here as nonuniqueness of solution is an inherent property of these types of problems. An analogy can be drawn with the algebraic quadratic equation that has two solutions. As the governing equations for fluid flow are nonlinear in

* Corresponding author. Tel.: +91 361 2582654; fax: +91 361 2690762.
E-mail addresses: d.perumal@iitg.ernet.in (D. Arumuga Perumal), anoop@iitg.ernet.in (A.K. Dass).

0898-1221/$ – see front matter © 2010 Elsevier Ltd. All rights reserved.
doi:10.1016/j.camwa.2010.03.053

nature, the possibility of their multiple solutions exists. In the case of lid-driven cavity flows multiple solutions are generally observed only if the walls move in pairs. In the case of parallel motion of two facing walls, multiple solutions are seen to exist only in cavities with aspect ratios other than one, i.e. in rectangular cavities. However, if the nonfacing walls of the cavity move, multiple steady solutions are observed even in square cavities [10].

Albensoeder et al. [6] were among the first to investigate the nonlinear regime and find multiple two-dimensional steady states in rectangular two-sided lid-driven cavities. They have found five and seven flow states in parallel and antiparallel motion respectively. Luo and Yang [11] numerically investigated flow bifurcation with and without heat transfer in a two-sided lid-driven rectangular cavity. More recently, the multiplicity of flow states induced by the motion of two-sided non-facing lid-driven square cavity flow and four-sided lid-driven cavity flow have been investigated by Wabha [10]. He found the critical Reynolds numbers of 1073 for the two-sided non-facing lid-driven square cavity and 129 for the four-sided lid-driven square cavity, beyond which it is possible for multiple steady states to exist.

So far conventional methods like Finite Volume Method (FVM), Finite Difference Method (FDM) etc. are being used to capture the multiple solutions for cavity flows. It is known that the Lattice Boltzmann Method is an alternative way of fluid simulation to conventional numerical methods for the Navier–Stokes equation. In LBM the nonlinearity of the Navier–Stokes equations is hidden in the quadratic velocity terms of the equilibrium distribution function. Therefore, LBM appears to have the ability to capture multiple solutions. However, so far no investigation is seen that uses LBM to capture multiple solutions. The present work is an attempt in that direction. This paper uses LBM to obtain multiple steady solutions in two- and four-sided lid-driven square cavities that involve movement of the nonfacing walls. Generally, to obtain multiple steady solutions through conventional techniques one uses an iterative solution procedure with different initial conditions. Here we also describe what strategy we employ to obtain multiple steady states through LBM.

This paper is organized in five sections. Section 2 describes LBM with single-relaxation-time scheme, associated boundary conditions and the two-dimensional nine-velocity lattice model. In Section 3 the credibility of the present LBM code is established through a comparison exercise with the results of two other works. Section 4 gives the strategy employed to capture the multiple-steady solutions and the results and discussion. Concluding remarks are made in Section 5.

2. Lattice Boltzmann Method and boundary conditions

In the last one and a half decade or so LBM has emerged as a new and effective approach of computational fluid dynamics (CFD) and it has achieved considerable success in simulating fluid flows and heat transfer [12–19]. The LBGK model with single relaxation time, which is a commonly used lattice Boltzmann method, is given by [15]

$$f_i(\mathbf{x} + \mathbf{c}_i\Delta t, t + \Delta t) - f_i(\mathbf{x}, t) = -\frac{1}{\tau}\left[f_i(\mathbf{x}, t) - f_i^{(0)}(\mathbf{x}, t)\right] \tag{1}$$

where f_i is the particle distribution function, $f_i^{(0)}(\mathbf{x}, t)$ is the equilibrium distribution function at $\mathbf{x}$, t, c_i is the particle velocity along the ith direction and τ is the time relaxation parameter. The $D2Q9$ square lattice used here has nine discrete velocities. A square lattice is used, each node of which has eight neighbours connected by eight links as shown in Fig. 1. Particles residing on a node move to their nearest neighbours along these links in unit time step. The particle velocities are defined as

$$\begin{aligned}
&\mathbf{c}_i = 0, \quad i = 0\\
&\mathbf{c}_i = (\cos(\pi/4(i-1)), \sin(\pi/4(i-1))), \quad i = 1, 2, 3, 4\\
&\mathbf{c}_i = \sqrt{2}(\cos(\pi/4(i-1)), \sin(\pi/4(i-1))), \quad i = 5, 6, 7, 8.
\end{aligned} \tag{2}$$

The macroscopic quantities such as density ρ and momentum density $\rho\mathbf{u}$ are obtained as velocity moments of the distribution function f_i as follows:

$$\rho = \sum_{i=0}^{N} f_i, \tag{3}$$

$$\rho\mathbf{u} = \sum_{i=0}^{N} f_i\mathbf{c}_i \tag{4}$$

where $N = 8$. In the $D2Q9$ square lattice, a suitable equilibrium distribution function that has been proposed is [15]

$$\begin{aligned}
f_i^{(0)} &= w_i\rho\left[1 - \frac{3}{2}\mathbf{u}^2\right], \quad i = 0\\
f_i^{(0)} &= w_i\rho\left[1 + 3(\mathbf{c}_i.\mathbf{u}) + 4.5(\mathbf{c}_i.\mathbf{u})^2 - 1.5\mathbf{u}^2\right], \quad i = 1, 2, 3, 4\\
f_i^{(0)} &= w_i\rho\left[1 + 3(\mathbf{c}_i.\mathbf{u}) + 4.5(\mathbf{c}_i.\mathbf{u})^2 - 1.5\mathbf{u}^2\right], \quad i = 5, 6, 7, 8
\end{aligned} \tag{5}$$

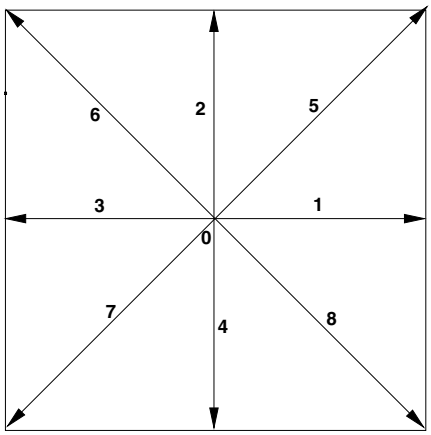

Fig. 1. Two-dimensional nine-velocity square lattice ($D2Q9$) model.

where the lattice weights are given by $w_0 = 4/9$, $w_{1-4} = 1/9$ and $w_{5-8} = 1/36$. The relaxation time which fixes the rate of approach to equilibrium is related to the viscosity by [15]

$$\tau = \frac{6\upsilon + 1}{2} \tag{6}$$

where υ is the kinematic viscosity measured in lattice units. It is seen that $\tau = 0.5$ is the critical value for ensuring a non-negative kinematic viscosity. Numerical instability can occur for a τ close to this critical value. This situation takes place at high Reynolds numbers. In this work Reynolds numbers up to 2000 in a lattice size of 201×201 are investigated.

Boundary conditions play a crucial role in LBM simulations. In this work bounce-back and equilibrium boundary condition [15] are applied on the stationary and moving walls respectively. In the bounce-back scheme, the particle distribution function at the wall lattice node is assigned to be the particle distribution function of its opposite direction. At the lattice nodes on the moving walls, flow-variables are re-set to their pre-assumed values at the end of every streaming-step. Initially, the equilibrium distribution function that corresponds to the flow-variables is assumed as the unknown distribution function for all nodes at $t = 0$. A uniform fluid density $\rho = 1.0$ is imposed initially. The solution procedure of the above LBM at each time step comprise streaming and collision steps, application of boundary conditions, calculation of particle distribution function followed by calculation of macroscopic variables.

3. Establishing the credibility of the LBM code

It may be noted that for the single lid-driven cavity some experimental, numerical and theoretical results exist, by reproducing which with LBM an insight about the appropriateness of the present boundary conditions can be gained. This knowledge is then utilized when applying the LBM to compute the two-sided and four-sided cavity flows. To lend credibility to the present LBM code its results for the single lid-driven cavity flow is first compared with those of two other works. Both of these numerically solves the two-dimensional Navier–Stokes equations in the stream function-vorticity form given by

$$\frac{\partial^2 \psi}{\partial x^2} + \frac{\partial^2 \psi}{\partial y^2} = -\omega \tag{7}$$

$$\frac{\partial \omega}{\partial t} + u\frac{\partial \omega}{\partial x} + \upsilon\frac{\partial \omega}{\partial y} = \frac{1}{Re}\left(\frac{\partial^2 \omega}{\partial x^2} + \frac{\partial^2 \omega}{\partial y^2}\right) \tag{8}$$

where ψ stands for stream function and ω stands for vorticity. In the first code, based on finite difference and developed by the present authors, all space derivatives are centrally differenced and ADI method is used for time integration to the steady state. The second work used for inter-code comparison is that of Ghia et al. [2]. To validate the present numerical method, the LBM code is used to compute the single lid-driven flow in a square cavity on a 161×161 lattice. A lid velocity of $U = 0.1$ is considered in this work. Fig. 2 depicts the streamline pattern at $Re = 1000$ obtained through LBM, which closely resembles those given by Ghia et al. [2] and by our FDM-based ADI code. Fig. 3 shows the comparison of steady-state u-velocity profile along a vertical line and υ-velocity profile along a horizontal line passing through the geometric centre of the cavity at $Re = 1000$. It is observed that the agreement between the present LBM results and those of the two works used for comparison is excellent. Thus the present LBM code stands validated.

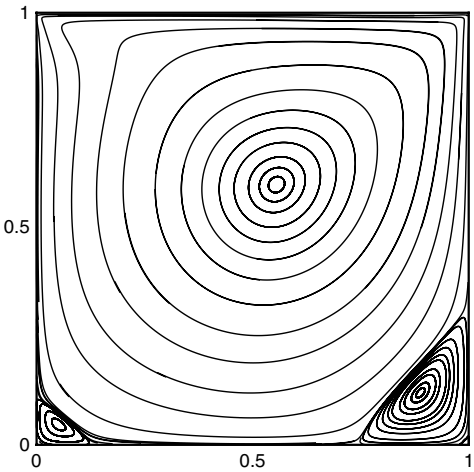

Fig. 2. Streamline pattern for the single-sided lid-driven cavity flow at $Re = 1000$.

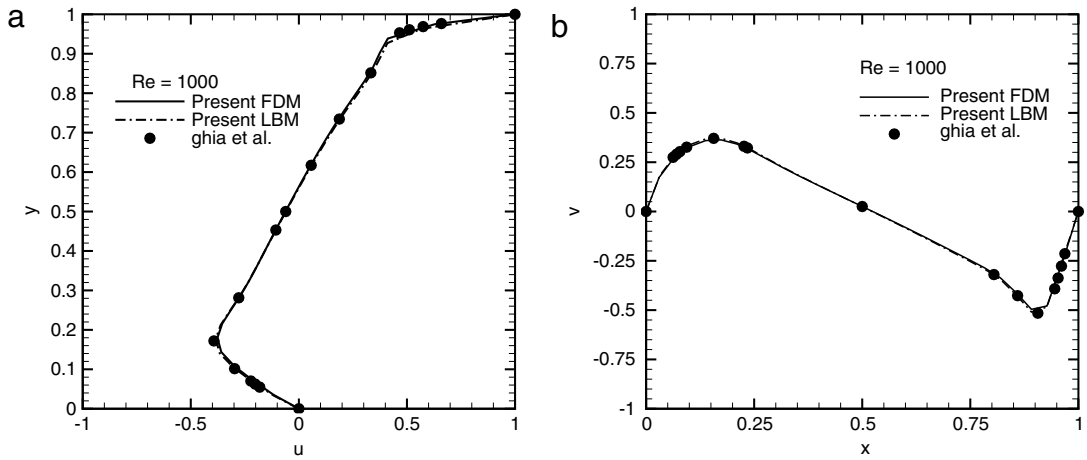

Fig. 3. Code validation: u—velocity along vertical centreline and v—velocity along horizontal centreline for single lid-driven square-cavity ($Re = 1000$).

4. Results and discussions

As already mentioned, in this work the multiple steady-flow states in two-sided non-facing lid-driven square cavity and four-sided lid-driven square cavity are first numerically captured using the Lattice Boltzmann Method. Unlike non-facing lid-driven cavities, for the parallel motion of two facing walls, the square cavity always gives a unique solution. However, for rectangular cavities with parallel motion of two walls multiple stable solutions exist [6]. Thus the present study is extended to two-dimensional rectangular cavity with parallel wall motion as well to capture multiple steady solutions. The method used to obtain multiple steady solutions in the LBM framework is also described.

4.1. Strategy used to obtain multiple steady solutions through LBM

In the conventional techniques like finite volume method one uses time-marching or other iterative procedures to obtain steady-flow solutions. Multiple solutions are obtained starting with different initial conditions that may be cleverly chosen to suit a certain type of final solution. Sometimes the choice of the sweeping direction for line-implicit iterative solver also determines the type of solution captured. In the Lattice Boltzmann Method, however, one deals with the time-evolution of the particle distribution functions and their relation with the macroscopic flow parameters is not immediately apparent. To capture multiple solutions in the cavity flow for a certain Reynolds number by Lattice Boltzmann Method, lid velocity U may be changed remaining within the incompressible Mach number limit. For the same Reynolds number, altering the value of the lid velocity, results in a change in the value of kinematic viscosity (see Eq. (6)) and hence a change in the relaxation time. All the multiple solutions given in the next subsections for several Reynolds numbers are obtained using various lid

Table 1
Locations of the vortex centres for two-sided lid-driven square cavity flow. The letters LPV, RPV, LSV and RSV denote Left Primary Vortex, Right Primary Vortex, Left Secondary Vortex and Right Secondary Vortex respectively.

Re	LPV		RPV		LSV		RSV	
	x	*y*	*x*	*y*	*x*	*y*	*x*	*y*
100	0.190	0.321	0.680	0.810	0.813	0.066	0.934	0.186
500	0.250	0.320	0.680	0.750	0.657	0.160	0.840	0.335
1000	0.252	0.321	0.675	0.744	0.658	0.199	0.780	0.343
1071	0.253	0.326	0.675	0.744	0.655	0.199	0.800	0.343

Table 2
Locations of the vortex centres for two-sided square cavity flow at $Re = 2000$.

Solution	LPV		RPV		LSV		RSV	
	x	*y*	*x*	*y*	*x*	*y*	*x*	*y*
Symmetry	0.254	0.326	0.675	0.746	0.655	0.199	0.799	0.344
Asymmetric (1)	0.353	0.426	0.781	0.827	0.862	0.421	0.895	0.583
Asymmetric (2)	0.178	0.226	0.575	0.653	0.421	0.106	0.583	0.143

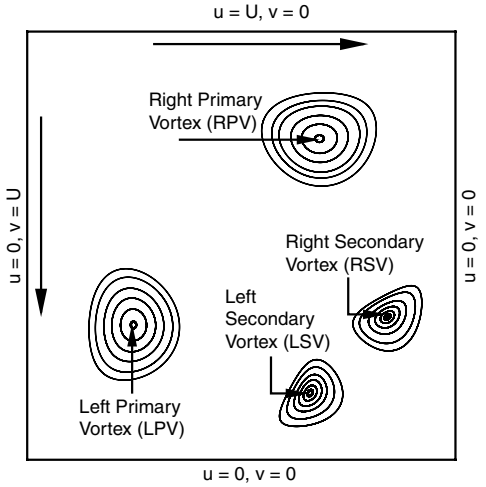

Fig. 4. Geometry and boundary conditions of the two-sided lid-driven square cavity flow.

velocities, and hence various relaxation times. Excellent agreement is obtained between the LBM and previous studies based on continuum approach.

4.2. Two-sided square cavity flow

The geometry and boundary conditions of the two-sided non-facing lid-driven square cavity flow is shown in Fig. 4. In this problem, while the upper cavity wall moves towards the right, the left cavity wall moves in the downward direction with an equal velocity. Fig. 5 depicts the streamlines of predicted flow patterns on a lattice size of 201×201 at Reynolds numbers 100, 500, 1000 and 1071 for the two-sided non-facing lid-driven square cavity. The solution demonstrates that symmetric solutions exist at all Reynolds numbers. The streamlines are diagonally symmetric for all the Reynolds numbers. The symmetric state, where two separate primary vortices are formed apparently adjacent to each of the moving walls. It is evident that for these relatively low Reynolds numbers two primary and two secondary vortices are formed. As the Reynolds number increases the secondary vortices grow bigger. Additional asymmetric flow patterns can be obtained above the critical Reynolds number of 1073 [10]. Here we choose a post-critical Reynolds number of 2000 to demonstrate the existence of multiple steady solutions. Fig. 6 depicts the streamline patterns for the two-sided non-facing lid-driven square cavity flow at $Re = 2000$. It is known that when the inertial effects become important at higher Reynolds numbers additional flow states arise in pairs that break the respective symmetry spontaneously. One symmetric state and two asymmetric states are identified in this problem. Beyond the critical Reynolds number at least one solution satisfies the symmetry geometry. These symmetric and asymmetric flow patterns agree well with those given by Wabha [10]. In Table 1 we present the locations of the left-primary, right-primary, left-secondary and right-secondary vortex centres for the pre-critical $Re = 100$, 500, 1000 and 1071. From this table and also from Fig. 5 all the vortex centres are seen to move towards the symmetry diagonal as

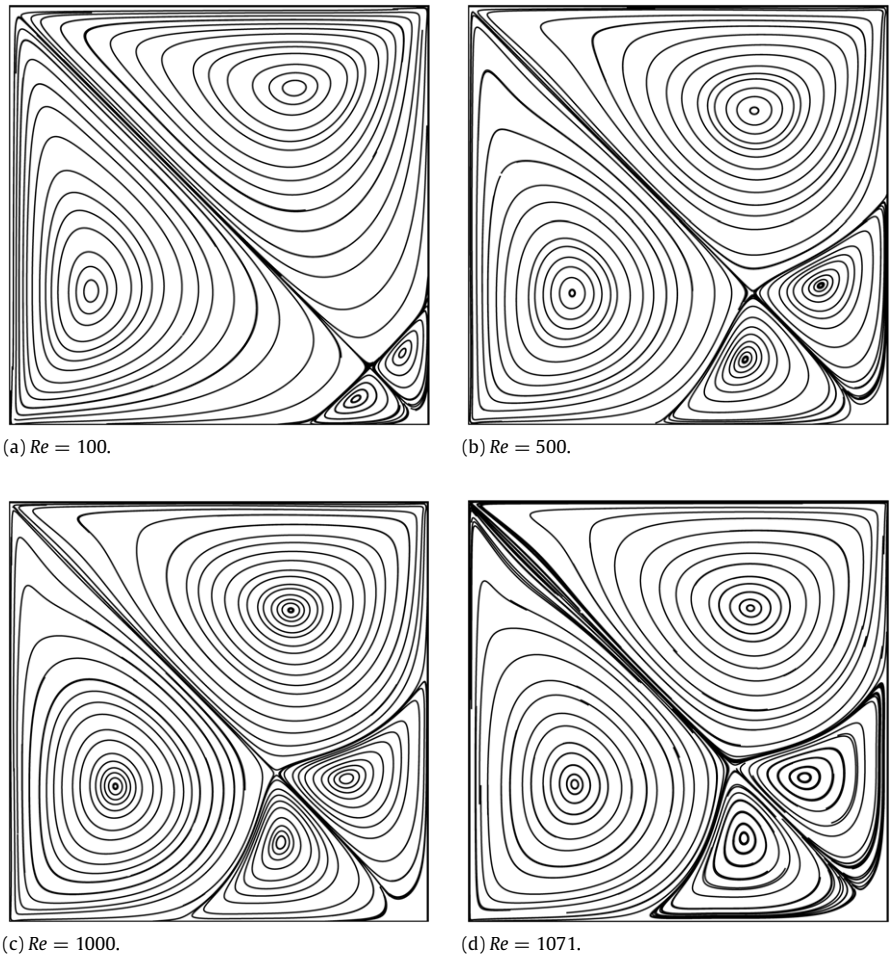

(a) $Re = 100$. (b) $Re = 500$.

(c) $Re = 1000$. (d) $Re = 1071$.

Fig. 5. Streamline pattern for two-sided lid-driven cavity flow at (a) $Re = 100$ (b) $Re = 500$ (c) $Re = 1000$ and (d) $Re = 1071$ on a 201×201 lattice.

Reynolds number increases. In Table 2 is presented the locations of the vortex centres for the symmetric and asymmetric solutions for the post-critical $Re = 2000$.

4.3. Four-sided square cavity flow

The geometry and boundary conditions of the four-sided lid-driven square cavity flow is shown in Fig. 7. In this problem, the upper cavity wall moves towards the right, the lower wall moves towards the left, while the right wall moves upwards, the left wall moves downwards with an equal velocity. Fig. 8 shows the streamlines of the predicted flow patterns on a lattice size of 161×161 for various Reynolds numbers ranging from low to critical ($Re = 10$, 100 and 127). The streamlines are diagonally symmetric with respect to both the cavity diagonals for all these pre-critical Reynolds numbers. Additional asymmetric flow patterns can be obtained above the critical Reynolds number of 129 [10]. To demonstrate the existence of multiple steady solutions a post-critical Reynolds number of 300 is chosen. Fig. 9 shows the streamline patterns for the four-sided lid-driven cavity flow at $Re = 300$. It is seen that when the inertial effects become important additional flow states arise in pairs that break the respective symmetry spontaneously. One symmetric state and two asymmetric states are identified for the four-sided lid-driven cavity flow at this Reynolds number. Beyond the critical Reynolds number at least one solution satisfies the symmetry geometry. Our symmetric and asymmetric flow patterns compare well with those given for the same problem by Wabha [10]. In Table 3, we present the locations of the left, right, top and bottom vortex centres (Fig. 8) for Reynolds numbers 10, 100 and 127. As the Reynolds number increases the vortex centres are seen coming closer to the diagonal joining the leading edges of the moving plates. The locations of the vortex centres for the symmetry solution at the post-critical $Re = 300$ (Fig. 9(a)) for the left, right, top and bottom vortices are (0.196, 0.481), (0.807, 0.532), (0.527, 0.806) and (0.481, 0.196) respectively. For one of the asymmetric solutions (Fig. 9(b)) the locations for the left, centre and right vortices are (0.123, 0.589), (0.498, 0.497) and (0.876, 0.409) respectively.

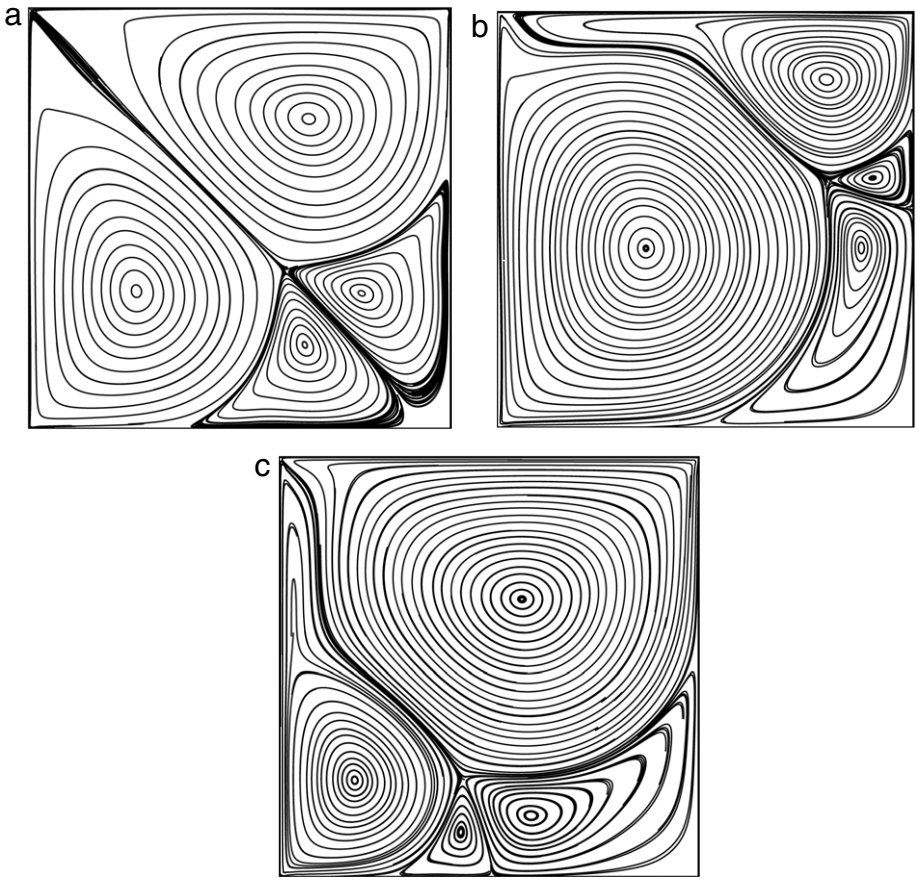

Fig. 6. Multiplicity of flow states for the two-sided non-facing lid-driven cavity flow at $Re = 2000$ on a 201×201 lattice. Shown are the streamline patterns of (a) symmetric solution, (b) asymmetric solution (1) and (c) asymmetric solution (2).

Table 3
Locations of the vortex centres for four-sided lid-driven square cavity flow. The letters LPV, RPV, TPV and BPV denote Left Primary Vortex, Right Primary Vortex, Top Primary Vortex and Bottom Primary Vortex respectively.

Re	LPV		RPV		TPV		BPV	
	x	*y*	*x*	*y*	*x*	*y*	*x*	*y*
10	0.150	0.490	0.849	0.510	0.510	0.850	0.490	0.149
100	0.160	0.450	0.840	0.550	0.550	0.840	0.450	0.160
127	0.170	0.450	0.830	0.550	0.548	0.830	0.449	0.168

4.4. Two-sided lid-driven rectangular cavity flow

The geometry and boundary conditions of the two-sided rectangular cavity with parallel wall motion is shown in Fig. 10. In this problem, both the left and right walls moves in the upward direction with an equal velocity. The flow geometry suggests that there is a flow pattern symmetric about the vertical centreline. This symmetric state exists for all Reynolds numbers. Multiple stable solutions, however, exist only for the higher values of Reynolds number. For the present flow configuration we demonstrate the existence of multiple solutions for a cavity aspect ratio of 0.75 and a Reynolds number of 600. Fig. 11 shows the multiple streamline patterns obtained by LBM using a 224×256 lattice structure. For this flow geometry five multiple stable solutions are obtained. Fig. 11(a) shows the weakly-stable symmetric solution, Fig. 11(b) shows one of the two weakly-stable asymmetric solutions and Fig. 11(c) shows one of the two strongly-stable asymmetric solutions. These results compare very well with those given for the same problem by Albensoeder et al. [6]. The locations of the vortex centres are not mentioned here as they keep changing with the cavity aspect ratio.

5. Conclusions

A single-relaxation-time model is used to carry out LBM computations to obtain multiple steady solutions for two- and four-sided lid-driven square cavities and two-sided rectangular cavities. To establish the credibility of the developed code

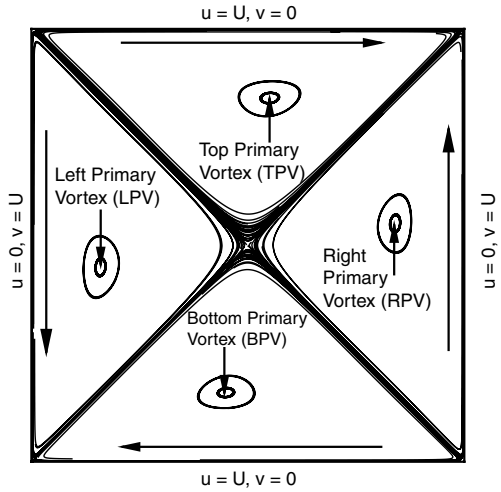

Fig. 7. Geometry and boundary conditions of the four-sided lid-driven square cavity flow.

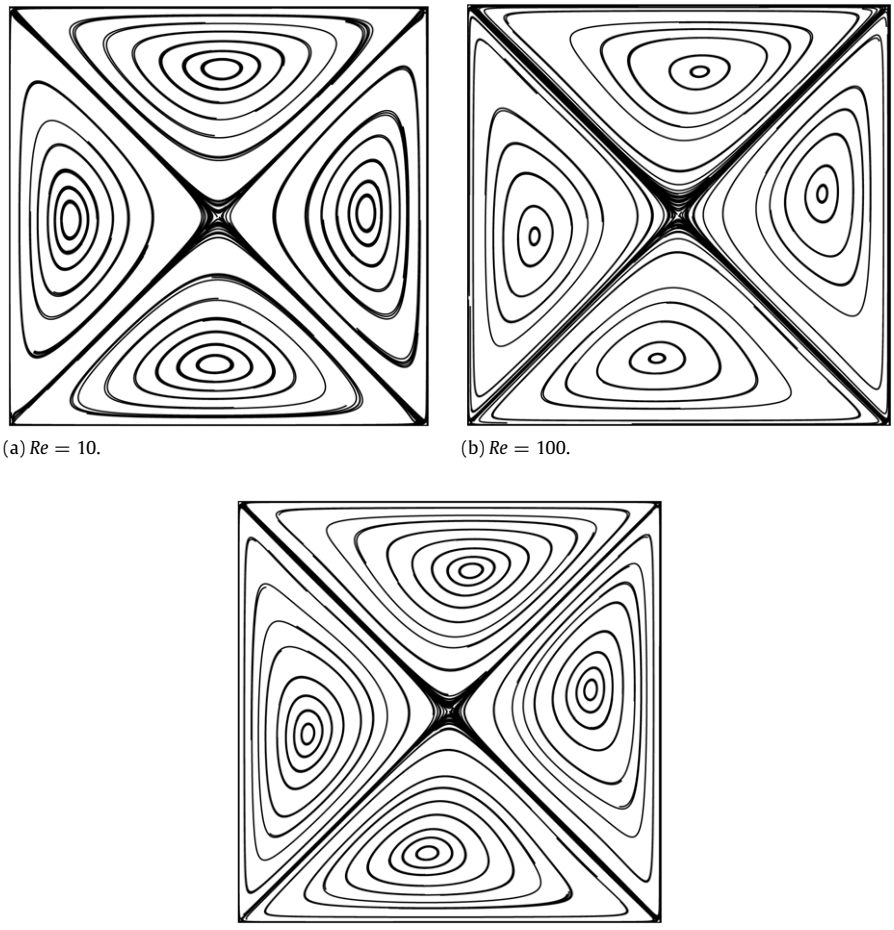

(a) $Re = 10$. (b) $Re = 100$.

(c) $Re = 127$.

Fig. 8. Streamline patterns for the four-sided square cavity flow at (a) $Re = 10$ (b) $Re = 100$ and (c) $Re = 127$ on a 161×161 lattice.

it is first used to compute the flow in a standard two-dimensional single lid-driven square cavity to demonstrate that the results closely agree with the results generated with a finite-difference-based code hand highly reliable existing results. After having thus gained confidence in the code it is then used to compute the flow in the two- and four-sided configurations

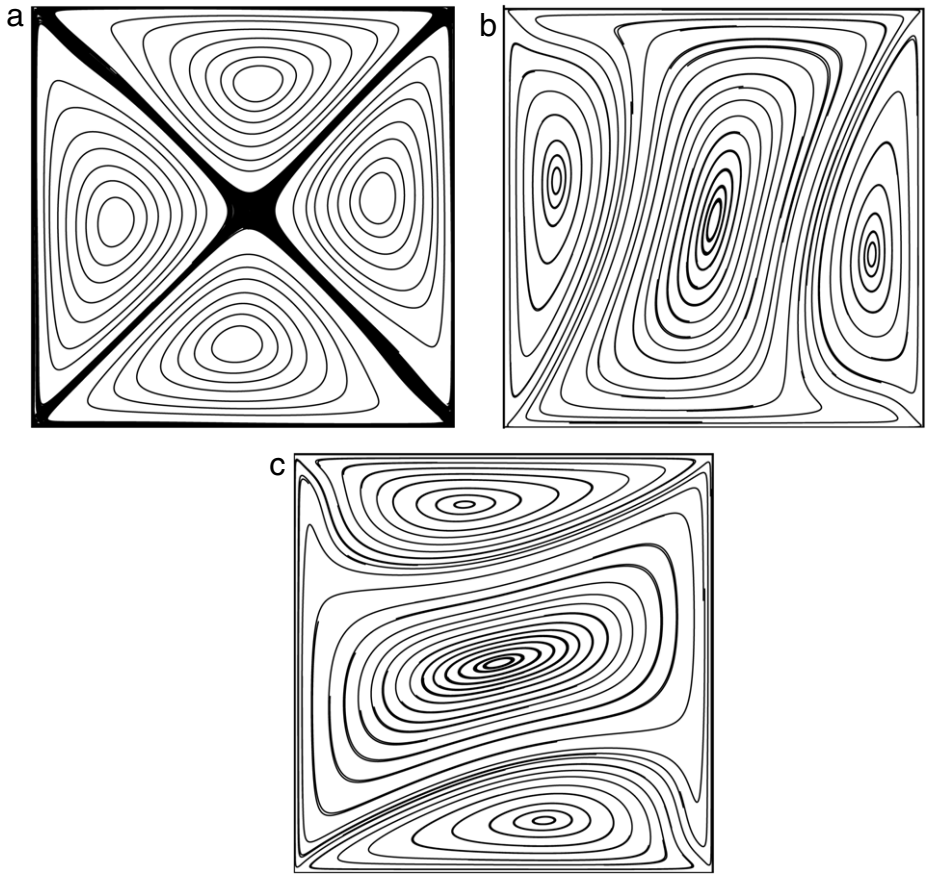

Fig. 9. Multiplicity of flow states for the four-sided square cavity flow at $Re = 300$ on a 161×161 lattice. Shown are the streamline patterns of (a) symmetric solution, (b) asymmetric solution (1) and (c) asymmetric solution (2).

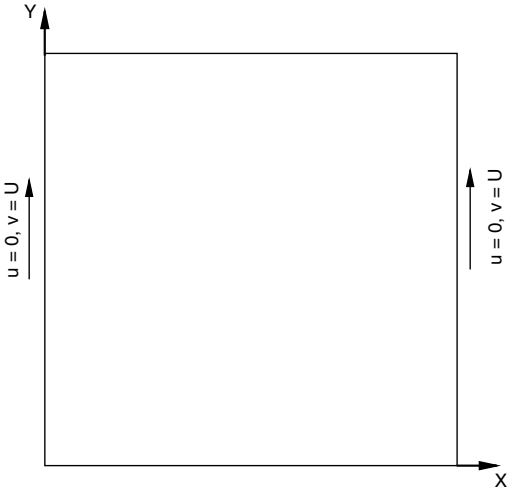

Fig. 10. Geometry and boundary conditions of the two-sided rectangular cavity flow.

mentioned above. These three flow configurations are fraught with interesting flow features in that they exhibit multiple steady solutions. The strategy used to obtain the multiple solutions for each of these geometries is necessarily different from the ones used in continuum-based techniques and this strategy is also described. Close comparison with existing results establish the validity of the multiple solutions. It may be recalled that nonlinear problems are known at times to give multiple solutions and the traditional mathematical concept of well-posedness does not apply here. For the first time the

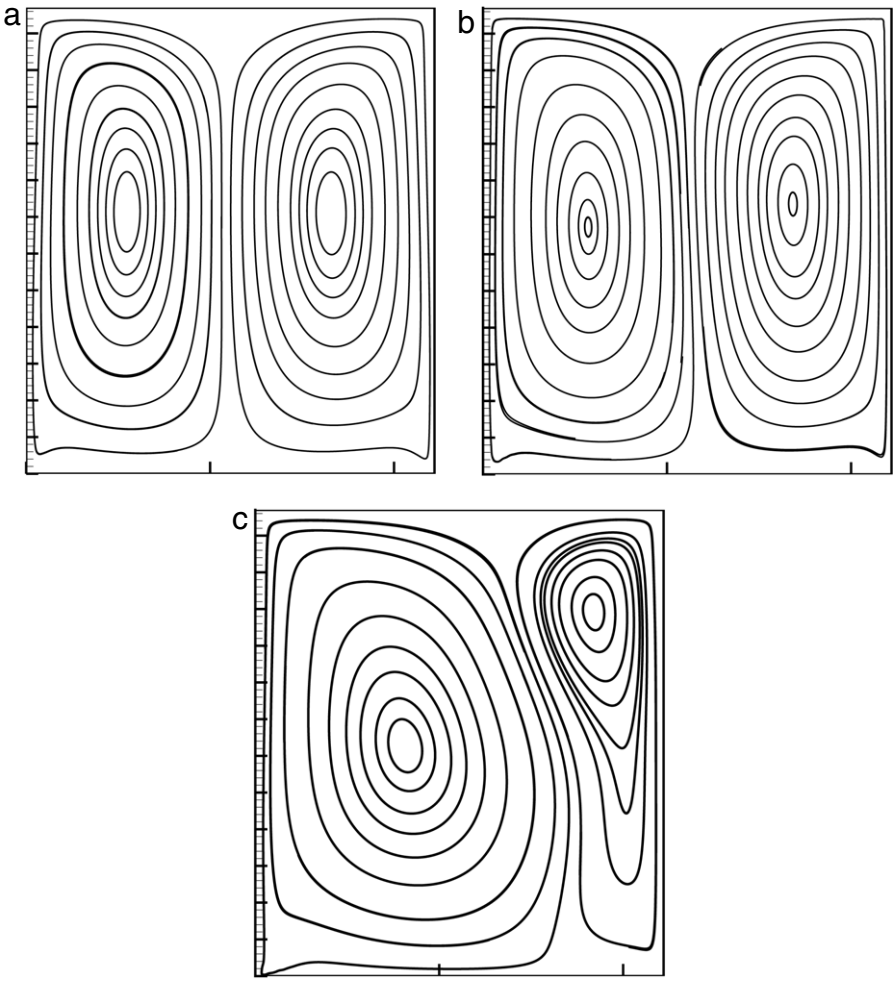

Fig. 11. Multiplicity of flow states for the two-sided rectangular cavity flow with parallel wall motion at $Re = 600$ (based on the shorter side) and aspect ratio of 0.875 on a 224×256 lattice. Shown are the streamline patterns of (a) symmetric solution, (b) weakly-stable asymmetric solution and (c) strongly-stable asymmetric solution.

ability and accuracy of the Lattice Boltzmann Method to obtain solutions to this peculiar class of problems is demonstrated. With this added ability it can be concluded that LBM, as an alternative to the continuum-based methods, holds very good promise in computational fluid dynamics.

References

[1] P.N. Shankar, M.D. Deshpande, Fluid mechanics in the driven cavity, Annual Review of Fluid Mechanics 32 (2000) 93–136.
[2] U. Ghia, K.N. Ghia, C.T. Shin, High-Re solutions for incompressible flow using the Navier–Stokes equations and a multigrid method, Journal of Computational Physics 48 (1983) 387–411.
[3] C.-H. Bruneau, M. Sadd, The 2D lid-driven cavity problem revisited, Computers & Fluids 35 (2006) 326–348.
[4] H.C. Kuhlmann, M. Wanschura, H.J. Rath, Flow in two-sided lid-driven cavities: non-uniqueness, instability and cellular structures, Journal of Fluid Mechanics 336 (1997) 267–299.
[5] H.C. Kuhlmann, M. Wanschura, H.J. Rath, Elliptic instability in two-sided lid-driven cavity flow, European Journal of Mech. B/Fluids 17 (1998) 561–569.
[6] S. Albensoeder, H.C. Kuhlmann, H.J. Rath, Multiplicity of steady two-dimensional flows in two-sided lid-driven cavities, Theoretical Computational Fluid Dynamics 14 (2001) 223–241.
[7] C.H. Blohm, H.C. Kuhlmann, The two-sided lid-driven cavity: experiments on stationary and time-dependent flows, Journal of Fluid Mechanics 450 (2002) 67–95.
[8] S. Albensoeder, H.C. Kuhlmann, Linear stability of rectangular cavity flows driven by anti-parallel motion of two-facing walls, Journal of Fluid Mechanics 458 (2002) 153–180.
[9] S. Albensoeder, H.C. Kuhlmann, H.J. Rath, Three-dimensional centrifugal-flow instabilities in the lid-driven cavity problem, Physics of Fluids 13 (2001) 121–135.
[10] E.M. Wabha, Multiplicity of states for two-sided and four-sided lid-driven cavity flows, Computers & Fluids 38 (2009) 247–253.
[11] W.-J. Luo, R.-J. Yang, Multiple fluid flow and heat transfer solutions in a two-sided lid-driven cavity, Int. Journal Heat and Mass Transfer 50 (2007) 2394–2405.
[12] D.A. Wolf-Gladrow, Lattice-Gas Cellular Automata and Lattice Boltzmann Models: An Introduction, Springer-Verlag, Berlin, Heidelberg, 2000.
[13] S. Chen, G.D. Doolen, Lattice Boltzmann method for fluid flows, Annual Review of Fluid Mechanics 30 (1998) 329–364.

[14] X. He, L.S. Luo, Theory of the lattice Boltzmann method: from the Boltzmann equation to the lattice Boltzmann equation, Physical Review E 56 (1997) 6811–6817.
[15] S. Hou, Q. Zou, S. Chen, G. Doolen, A.C. Cogley, Simulation of cavity flow by the lattice Boltzmann method, Journal of Computational Physics 118 (1995) 329–347.
[16] Y.G. Lai, C.L. Lin, J. Huang, Accuracy and efficiency study of a lattice Boltzmann method for steady-state flow simulations, Numerical Heat Transfer Part B 39 (2001) 21–43.
[17] Z. Guo, C. Zheng, B. Shi, An extrapolation method for boundary conditions in lattice Boltzmann method, Physics of Fluids 14 (6) (2002) 2007–2010.
[18] D. Arumuga Perumal, A.K. Dass, Simulation of flow in two-sided lid-driven square cavities by the lattice Boltzmann method, in: Advances in Fluid Mechanics VII, May 21–23, 2008, New Forest, UK, pp. 45–54.
[19] S. Geller, M. Krafczyk, J. Tolke, S. Turek, J. Hron, Benchmark computations based on lattice Boltzmann, finite element and finite volume methods for laminar flows, Computers & Fluids 35 (2006) 888–897.